

Ultrasonographic assessment of the lateral pterygoid muscle for BoNT-A injection

Hyungkyu Bae¹ | Yeon-Hee Lee² | Soo-Bin Kim^{1,3} | Kyung-Seok Hu¹ | Hee-Jin Kim^{1,4} 

¹Division in Anatomy and Developmental Biology, Department of Oral Biology, Human Identification Research Institute, BK21 FOUR Project, Yonsei University College of Dentistry, Seoul, Republic of Korea

²Department of Orofacial Pain and Oral Medicine, Kyung Hee University Dental Hospital, Kyung Hee University, Seoul, Republic of Korea

³Department of Oral Anatomy, Institute of Biomaterial Implant, College of Dentistry, Wonkwang University, Iksan, Republic of Korea

⁴Department of Materials Science and Engineering, College of Engineering, Yonsei University, Seoul, Republic of Korea

Correspondence

Hee-Jin Kim, Room 601, Department of Oral Biology, Yonsei University College of Dentistry, 50 Yonsei-ro, Seodaemun-gu, Seoul 03722, Republic of Korea.

Email: hjk776@yuhs.ac

Funding information

Yonsei University College of Dentistry

Abstract

The upper head of the lateral pterygoid muscle (LPM) is known to insert into the capsule of the temporomandibular joint and articular disc, and therefore its relationship with temporomandibular disorders (TMD) has been consistently suggested. The aim of the study was to determine the anatomical features of the LPM using ultrasonographic (US) imaging. Around 120 hemifaces from 60 healthy Korean volunteers were included in this study. US images were taken with the subject's mouth 2 cm open. The transducer was placed at a position where the infratemporal fossa could be observed through the mandibular notch, and its position was recorded. The locations of the coronoid process (CorP), lateral margin of the condylar process (ConP), and midpoint of CorP and ConP (MP) were measured with reference to the ala-tragus line. The thicknesses of the skin and subcutaneous tissue, the masseter muscle, the temporalis muscle, and the depth of the LPM were measured at the MP. The masseter muscle, temporalis muscle, and LPM were observed in all cases and located in order from superficial to deep. The MP was located 39.6 ± 3.3 mm anterior and 7.8 ± 1.6 mm inferior to the tragus. The thicknesses of the skin and subcutaneous tissue, the masseter muscle, the temporalis muscle, and the depth of the LPM at the MP were 9.7 ± 1.0 , 10.3 ± 1.3 , 10.9 ± 1.6 , and 30.9 ± 1.9 mm, respectively. The information reported in this study may be useful for determining the location of the LPM and adjacent anatomical structures in TMD patients and provide accurate and safe injection guidelines.

KEY WORDS

BoNT-A injection, cadaver, lateral pterygoid muscle, temporomandibular disorder

1 | INTRODUCTION

The lateral pterygoid muscle (LPM) is a masticatory muscle located within the infratemporal fossa, responsible for the protraction, depression, and unilateral movements of the mandible. This muscle consists of two heads, upper and lower, which originate from the sphenoid

bone and insert into the mandible (Murray et al., 2004; Murray et al., 2007). Some anatomical and histological studies have revealed that some fibers of the LPM are continuously attached to the articular disc and fibrous capsule of the temporomandibular joint (TMJ) (Fujita et al., 2001; Heylings et al., 1995; Peterson & Naidoo, 1996). Given the LPM's involvement in the functional movements of the mandible

This is an open access article under the terms of the [Creative Commons Attribution-NonCommercial-NoDerivs](#) License, which permits use and distribution in any medium, provided the original work is properly cited, the use is non-commercial and no modifications or adaptations are made.

© 2024 The Author(s). *Clinical Anatomy* published by Wiley Periodicals LLC on behalf of American Association of Clinical Anatomists and British Association of Clinical Anatomists.

and its direct connection to the TMJ, its relationship with temporomandibular disorder (TMD) has been steadily suggested (Fujita et al., 2001; Juniper, 1984; Wongwatana et al., 1994).

Numerous studies have explored the management of TMD through the injection of botulinum toxin into the LPM. Since the LPM is located deep within the infratemporal fossa and is covered by other major anatomical structures, including the masseter muscle and mandibular ramus, the accuracy of the traditional approach of blind injection is questionable. Consequently, methods of approaching the LPM under the guidance of computed tomography (CT) or magnetic resonance imaging (MRI) have been proposed (Pons et al., 2019; Yoshida, 2018). These methods enable precise injections but are complex, time-consuming, and costly. Few studies have suggested the possibility of accessing the infratemporal fossa and LPM through the mandibular notch (or sigmoid notch) under US guidance (Anugeraha et al., 2020; Chen et al., 2018; Qin & Xie, 2020). US can visualize anatomical structures in real-time and allow their quantitative measurement, making it suitable for identifying the deeply positioned LPM. Additionally, the process is relatively simple and cost-effective. However, since the space, consisting of a zygomatic arch and a mandibular notch is small and difficult to locate, an approach protocol needs to be established. In addition, locating and analyzing the LPM and its surrounding structures under US guidance has not yet been well studied.

Ultrasound offers the capability to observe dynamic changes in the anatomical structures in real-time, providing an intuitive understanding of the adjacent structures. The Doppler mode of US can identify the location and type of blood vessels by analyzing blood flow within soft tissues. Additionally, US facilitates the analysis of z-axis (depth) information of the anatomical structures, which was relatively limited in traditional dissection studies.

US guidance has recently been utilized to administer injections while accurately examining the musculoskeletal areas (Church et al., 2017; Çiftel et al., 2013; Ruiz Santiago et al., 2019; Von Coelln et al., 2008). By enabling real-time visualization of target structures and needle positions, US is utilized for precise injections into small muscles or specific sites. The ability to visualize anatomical variations provides safety and reliability during US-guided injections (Bae et al., 2020; Bae et al., 2023; Choi et al., 2021).

In light of the challenges associated with minimally invasive procedures for the LPM, a thorough anatomical understanding and the implementation of US-guided injections represent a novel approach to addressing these issues. Therefore, our study aimed to identify the clinical anatomy of the LPM and surrounding structures under US guidance, and thereby propose safe guidelines for minimally invasive procedures involving the masticatory muscles.

2 | MATERIALS AND METHODS

The study was conducted in accordance with the guidelines of the Declaration of Helsinki and was approved by the Institutional Review Board of Yonsei University Dental Hospital (IRB no. 2-2023-0050).

A total of 120 hemifaces from 60 healthy young Korean volunteers (60 females; age 36.7 ± 3.5 years [mean \pm SD]) were included

in this study. The exclusion criteria were as follows: patients with (1) TMJ disorder; (2) obvious facial asymmetry; (3) a history of plastic surgery; and (4) a history of receiving botulinum toxin injection within the preceding 6 months. Written informed consent was obtained from each participant prior to the study, with a full explanation of potential side effects and the option to withdraw from the study at any time.

A real-time, two-dimensional B-mode ultrasound device with a high-frequency (15 MHz) linear transducer (E-CUBE 15 PLATINUM, ALPINION, Seoul, Korea) was utilized to obtain US images. All the landmarks and reference lines were marked on the skin using waterproof eyeliner prior to US analysis. A thick layer of ultrasound gel (SONO JELLY, MEDITOP Corporation, Youngjin, Korea) was applied to the skin surface to ensure optimal transducer-skin contact and to prevent compression of the soft tissues by the transducer. At each reference point and line, the transducer was positioned so that the left side of the image indicated the direction of the medial or superior. US images were obtained with the volunteer in an upright seated position. After the US procedure, cleaners and moisturizers were provided for patient convenience.

US analysis was performed with the patient's mouth open 2 cm to facilitate access to the LPM through the mandibular notch. The transducer was initially positioned perpendicular to the skin. Then, the transducer was aligned and rotated to find the location where the coronoid and condylar processes were simultaneously observed on the same plane. The US image was taken at this location, the location of the transducer was recorded, and a photograph of the side view of the volunteer was taken. Based on the locations of the coronoid process and condylar process on the US image and the location of the transducer in the side view photograph, the following reference points were defined and their positions were measured with reference to the ala-tragus line (Figure 1A): (1) location of the coronoid process (designated as CorP), (2) location of the condylar process (designated as ConP), and (3) the midpoint between CorP and ConP (designated as MP). The thicknesses of the skin and subcutaneous layer, masseter muscle, and temporalis muscle, and the distance from the skin to the LPM at the MP were measured using the ImageJ program (Figure 1B,C) (National Institutes of Health, Bethesda, MD, USA).

3 | RESULTS

The masseter, temporalis, and LPM were observed through the mandibular notch in all cases and located in order from the most superficial to the deepest (Figure 2). The mean thicknesses of the skin and subcutaneous layer, masseter muscle, and temporalis muscle, and depth of the LPM were 9.7 ± 1.0 , 10.3 ± 1.3 , 10.9 ± 1.6 , and 30.9 ± 1.9 mm, respectively, at the MP (Table 1, Figure 3).

The location and the distribution of the CorP, MP, and ConP are listed in Table 2 and illustrated in Figure 4. The CorP was located 54.0 ± 3.9 mm anterior to the tragus and 10.7 ± 2.8 inferior to the ala-tragus line; the corresponding locations for MP and ConP were 39.6 ± 3.3 and 7.8 ± 1.6 mm, and 25.2 ± 3.0 mm and 4.9 ± 1.9 mm, respectively.

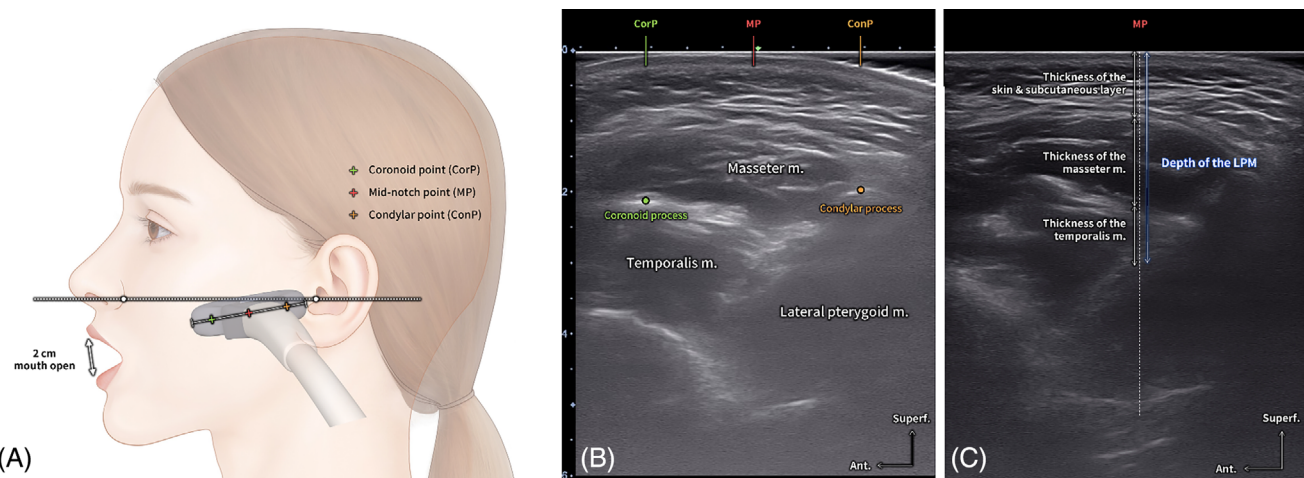


FIGURE 1 Ultrasonographic imaging and measurement protocol of lateral pterygoid muscle (LPM). (A) The location where the coronoid process and the condylar process were simultaneously observed at the same plane. (B) Ultrasonography of the LPM and infratemporal fossa (B mode, 15-MHz linear transducer). (C) Measurement of the thickness of the skin and subcutaneous layer, the thickness of the masseter muscle, and the temporalis muscle, and the distance from the skin to the LPM at the point MP.

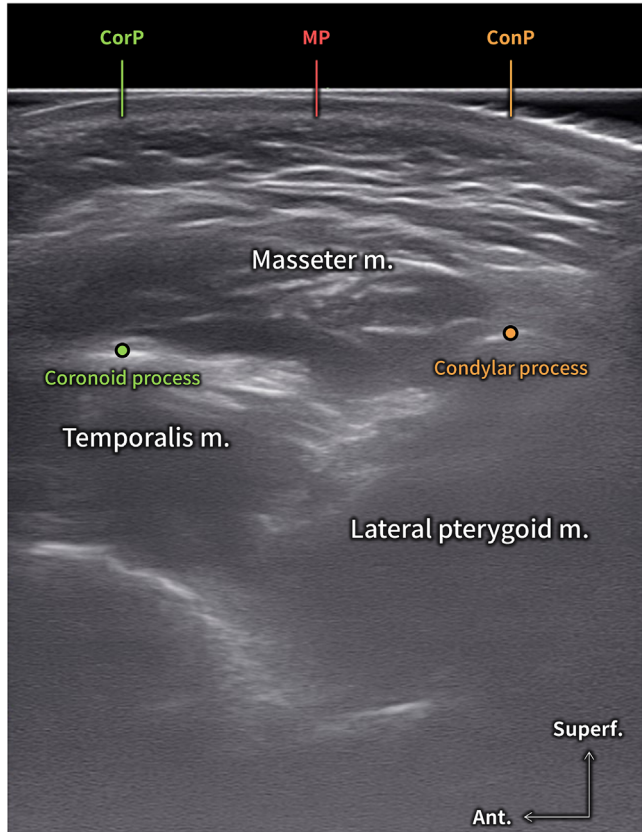


FIGURE 2 Ultrasonography of the lateral pterygoid muscle through the mandibular notch, B mode (transverse view, 15 MHz by linear transducer). CorP, location of the coronoid process; ConP, location of the condylar process; MP, midpoint between CorP and ConP.

4 | DISCUSSION

Several decades have passed since the botulinum toxin injections were first applied to the LPM for therapeutic purposes. Despite their potential benefits, these injections were not popularly implemented due to the LPM's deep and complex location. Several studies have tried to overcome these difficulties through the manufactured guide

using CT and MRI (Pons et al., 2019; Yoshida, 2018). While these methods can accurately target the intended structure, they are inherently complex, time-consuming, and costly.

The proposed approaches for LPM injection are primarily divided into extraoral and intraoral methods. Among them, the extraoral approach utilizes the space formed by the zygomatic arch and mandibular notch as a "window" for the injection (Altaweel et al., 2019). In this

TABLE 1 The mean thicknesses of the skin and subcutaneous layer, masseter muscle, and temporalis muscle, and depth of the lateral pterygoid muscle (LPM) at MP.

| MP | Skin and Subcutaneous layer | Masseter muscle | Temporalis muscle | Depth to LPM |
|---------------|-----------------------------|-----------------|-------------------|----------------|
| Mean \pm SD | 9.7 \pm 1.0 | 10.3 \pm 1.3 | 10.9 \pm 1.6 | 30.9 \pm 1.9 |
| Minimum | 8.0 | 7.8 | 8.8 | 27.9 |
| Maximum | 10.8 | 13.2 | 13.2 | 33.0 |

Note: The data are expressed as mean \pm SD values (mm).

Abbreviations: ConP, the location of the condylar process; CorP, the location of the coronoid process; MP, the midpoint between CorP and ConP.

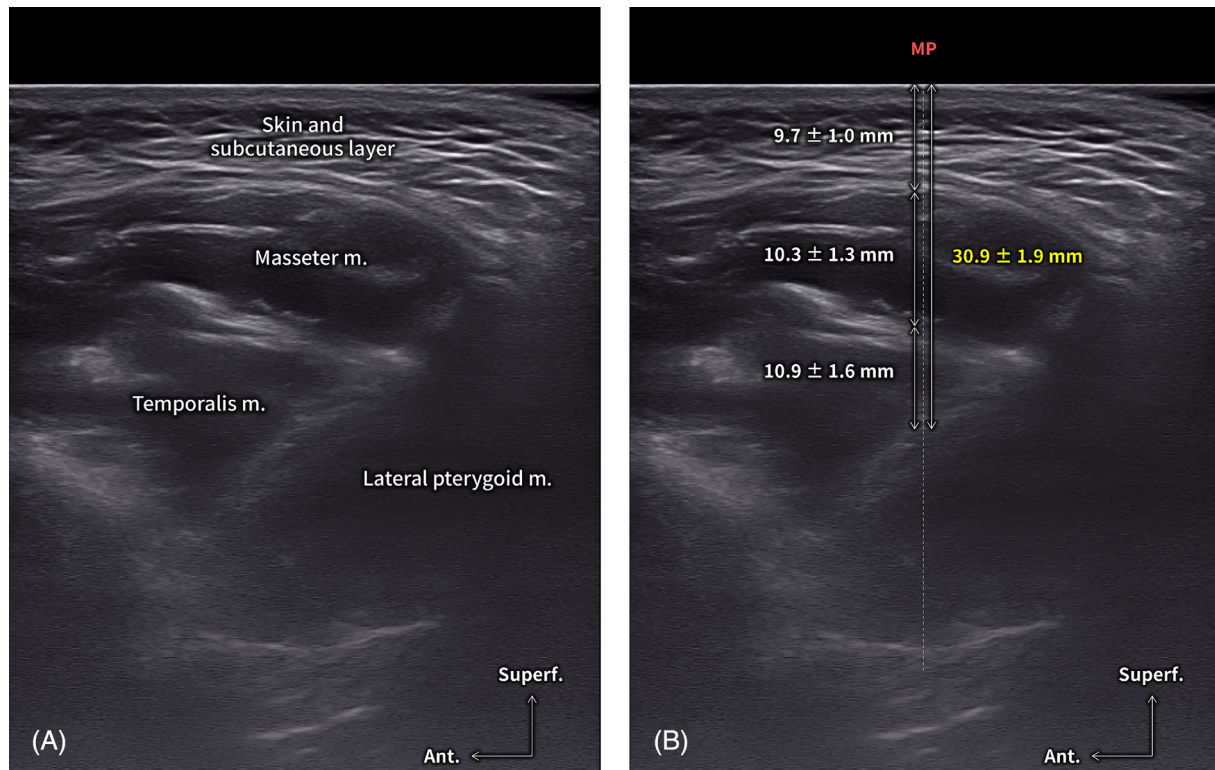


FIGURE 3 Ultrasonographic measurements at MP, B mode (transverse view, 15 MHz by linear transducer). (A) Ultrasonography of the lateral pterygoid muscle (LPM) through the mandibular notch. (B) The mean thicknesses of the skin and subcutaneous layer, masseter muscle, temporalis muscle, and depth of the LPM were 9.7 ± 1.0 , 10.3 ± 1.3 , 10.9 ± 1.6 , and 30.9 ± 1.9 mm, respectively at MP. CorP, location of the coronoid process; ConP, location of the condylar process; MP, midpoint between CorP and ConP.

TABLE 2 The location and the distribution of the CorP, MP, and ConP reference to the ala-tragus line.

| | CorP | MP | ConP |
|----------------|----------------|----------------|----------------|
| <i>x</i> -axis | | | |
| Mean \pm SD | 54.0 \pm 3.9 | 39.6 \pm 3.3 | 25.2 \pm 3.0 |
| Minimum | 44.4 | 30.0 | 11.7 |
| Maximum | 66.4 | 50.1 | 34.0 |
| <i>y</i> -axis | | | |
| Mean \pm SD | 10.7 \pm 2.8 | 7.8 \pm 1.6 | 4.9 \pm 1.9 |
| Minimum | 5.5 | 3.6 | 0.7 |
| Maximum | 22.7 | 15.9 | 9.8 |

Note: The data are expressed as mean \pm SD values (mm).

Abbreviations: ConP, the location of the condylar process; CorP, the location of the coronoid process; MP, the midpoint between CorP and ConP.

study, we investigated the location of this mandibular notch space to provide an accurate guideline for an extraoral approach. The MP, which can be assumed as the midpoint of the mandibular notch space, was located 39.6 ± 3.3 mm anterior and 7.8 ± 1.6 mm inferior to the tragus.

US technology enables real-time observation of anatomical structures and has the advantage of simple operation and process, low cost, and minimal side effects. As the performance of ultrasonic devices has improved, the resolution of US images has increased, and research and analysis targeting small anatomical structures that had not been attempted before are being actively conducted (Choi et al., 2019; Lee et al., 2019). In cases where the target anatomical structures are challenging to visually identify or where critical anatomical structures are in close proximity, US injection techniques can be employed as a precise method for targeting the intended injection site.

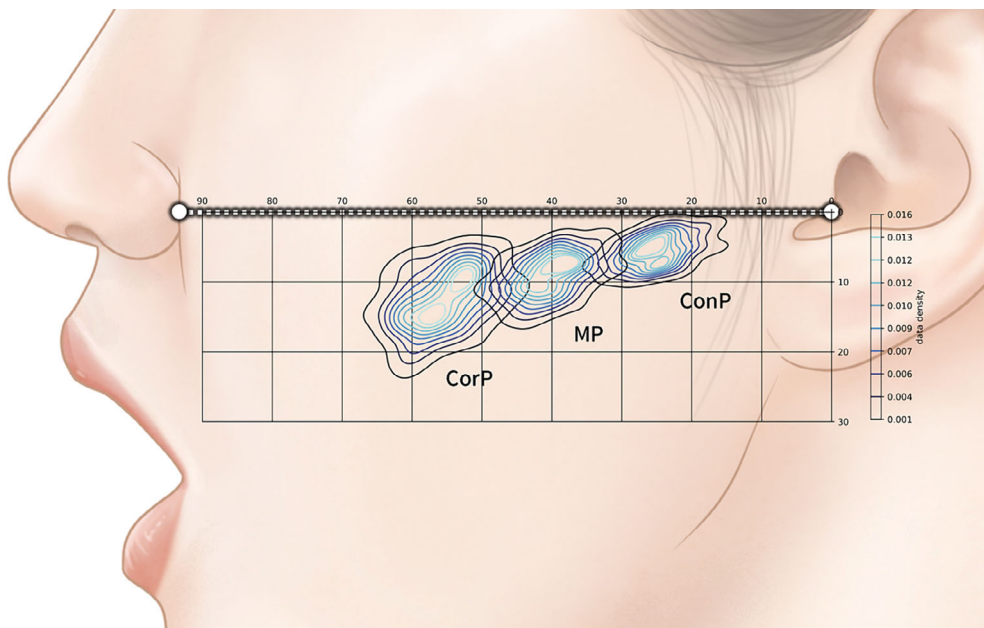


FIGURE 4 Distribution of the reference points relative to the ala-tragus line. CorP, location of the coronoid process; ConP, location of the condylar process; MP, midpoint between CorP and ConP.

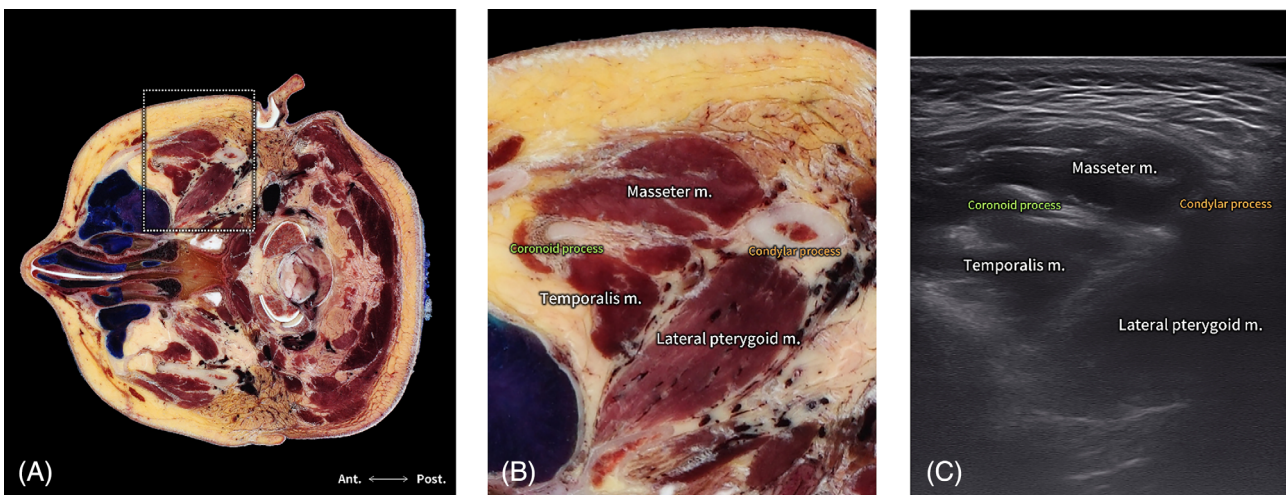


FIGURE 5 Comparison between cross-section image and ultrasonographic (US) image of lateral pterygoid muscle. (A) Cross-section image of the head at the level of mandibular notch. (B) Magnified cross-section image. (C) US image obtained at the level of mandibular notch. Cross-section was adapted from Visible Korean human co-produced by KISTI and Ajou University School of Medicine. (Park et al., 2005)

In this study, US images obtained from the MP exhibited a consistent anatomical features. Deep to the skin and subcutaneous layer, the masseter muscle was located most superficially. The lateral surfaces of the coronoid process and condylar process were observed as hyperechoic short lines. At a deeper position, the temporalis muscle was located anteriorly and superficially, whereas the LPM was located posteriorly and deeply. The position of each structure can be confirmed once again by comparing them with the cross-sectional image of the head (Park et al., 2005) (Figure 5).

According to the measurement results, the distance from the skin to the LPM at the MP was 30.9 ± 1.9 mm. Therefore, in order to access the LPM at this location, the injection should be performed at a depth of at least 3 cm. However, as can be seen from the US images,

the LPM is not located parallel to the skin. This may vary depending on the morphology of the individual's facial contour, and the depth of the muscle may vary if the injection point is moved a little from the MP. Therefore, for clinical application, it is recommended to confirm the precise location of MP and LPM through the US analysis before the injection.

In addition to the LPM, the US image at this location shows the upper part of the masseter and the tendinous part of the temporalis. For indications that require an approach to these structures, the results of the present study will be helpful.

The approach through the mandibular notch may offer a precise and easily applicable method for LPM injection. Nevertheless, the maxillary artery, which courses along the surface of the LPM, is a

structure that requires meticulous attention during injection administered via the mandibular notch. According to Lepić et al. (2019), US measurements taken from the mandibular notch indicated that the maxillary artery could be observed through Doppler mode coursing at a depth of approximately 2.4 mm (2.20–2.60 mm). Therefore, for a safer injection, it is recommended to perform US injections after confirming the depth through US examination and determining the position of the maxillary artery rather than relying solely on the depth information provided in this study.

ACKNOWLEDGMENTS

This study was supported by the Yonsei University College of Dentistry Fund (No. 6-2023-0002). The authors thank Hyewon Hu (M.F.A.) of Yonsei University, Graduate School for delicate illustrations of the figures. The authors also thank Michelle Hwang from University of Melbourne for her revision for the English translation in the manuscript.

CONSENT STATEMENT

Written informed consent was obtained from each participant prior to the study, with a full explanation of potential side effects and the option to withdraw from the study at any time.

ORCID

Hee-Jin Kim  <https://orcid.org/0000-0001-5572-1364>

REFERENCES

Altawee, A. A., Elsayed, S. A.-H., Baiomy, A. A. B. A., Abdelsadek, S. E., & Hyder, A. A. (2019). Extraoral versus intraoral botulinum toxin type a injection for management of temporomandibular joint disc displacement with reduction. *Journal of Craniofacial Surgery*, 30, 2149–2153.

Anugerah, A., Nguyen, K., & Nader, A. (2020). Technical considerations for approaches to the ultrasound-guided maxillary nerve block via the pterygopalatine fossa: a literature review. *Regional Anesthesia & Pain Medicine*, 45, 301–305.

Bae, H., Choi, Y. J., Lee, K. L., Gil, Y. C., Hu, K. S., & Kim, H. J. (2023). The deep temporal arteries: Anatomical study with application to augmentations procedures of the Temple. *Clinical Anatomy*, 36, 386–392.

Bae, H., Kim, J., Seo, K. K., Hu, K.-S., Kim, S.-T., & Kim, H.-J. (2020). Comparison between conventional blind injections and ultrasound-guided injections of botulinum toxin type a into the masseter: A clinical trial. *Toxins*, 12, 588.

Chen, Y., Chang, P.-H., Chang, K.-V., Wu, W.-T., & ÖzéAKAR, L. (2018). Ultrasound guided injection for medial and lateral pterygoid muscles: A novel treatment for orofacial pain. *Medical Ultrasonography*, 20, 115.

Choi, D.-Y., Bae, H., Bae, J.-H., Kim, H.-J., & Hu, K.-S. (2021). Effective locations for injecting botulinum toxin into the mentalis muscle; cadaveric and ultrasonographic study. *Toxins*, 13, 96.

Choi, Y.-J., Lee, K.-W., Gil, Y.-C., Hu, K.-S., & Kim, H.-J. (2019). Ultrasoundographic analyses of the forehead region for injectable treatments. *Ultrasound in Medicine & Biology*, 45, 2641–2648.

Church, J. T., Gadepalli, S. K., Talishinsky, T., Teitelbaum, D. H., & Jarboe, M. D. (2017). Ultrasound-guided intraspincteric botulinum toxin injection relieves obstructive defecation due to Hirschsprung's disease and internal anal sphincter achalasia. *Journal of Pediatric Surgery*, 52, 74–78.

Çiftéi, T., Akinci, D., Yurtutan, N., & Akhan, O. (2013). US-guided botulinum toxin injection for excessive drooling in children. *Diagnostic and Interventional Radiology*, 19, 56.

Fujita, S., Iizuka, T., & Dauber, W. (2001). Variation of heads of lateral pterygoid muscle and morphology of articular disc of human temporomandibular joint—anatomical and histological analysis. *Journal of Oral Rehabilitation*, 28, 560–571.

Heylings, D. J., Nielsen, I. L., & McNeill, C. (1995). Lateral pterygoid muscle and the temporomandibular disc. *Journal of Orofacial Pain*, 9, 9–16.

Juniper, R. P. (1984). Temporomandibular joint dysfunction: A theory based upon electromyographic studies of the lateral pterygoid muscle. *British Journal of Oral and Maxillofacial Surgery*, 22, 1–8.

Lee, H. J., Choi, Y. J., Lee, K. W., Hu, K. S., Kim, S. T., & Kim, H. J. (2019). Ultrasonography of the internal architecture of the superficial part of the masseter muscle in vivo. *Clinical Anatomy*, 32, 446–452.

Lepić, T., Lepić, M., & Mandić-Rajčević, S. (2019). Ultrasonographic assessment of the maxillary artery and middle meningeal artery in the infratemporal fossa. *Journal of Clinical Ultrasound*, 47, 405–411.

Murray, G., Phanachet, I., Uchida, S., & Whittle, T. (2004). The human lateral pterygoid muscle: A review of some experimental aspects and possible clinical relevance. *Australian Dental Journal*, 49, 2–8.

Murray, G. M., Bhutada, M., Peck, C. C., Phanachet, I., Sae-Lee, D., & Whittle, T. (2007). The human lateral pterygoid muscle. *Archives of Oral Biology*, 52, 377–380.

Park, J. S., Chung, M. S., Hwang, S. B., Lee, Y. S., Har, D.-H., & Park, H. S. (2005). Visible Korean human: Improved serially sectioned images of the entire body. *IEEE Transactions on Medical Imaging*, 24, 352–360.

Peterson, L. J., & Naidoo, L. C. D. (1996). Lateral pterygoid muscle and its relationship to the meniscus of the temporomandibular joint. *Oral Surgery, Oral Medicine, Oral Pathology, Oral Radiology, and Endodontology*, 82, 4–9.

Pons, M., Meyer, C., Euvrard, E., Weber, E., Sigaux, N., & Louvrier, A. (2019). MR-guided navigation for botulinum toxin injection in the lateral pterygoid muscle. First results in the treatment of temporomandibular joint disorders. *Journal of Stomatology, Oral and Maxillofacial Surgery*, 120, 188–195.

Qin, X., & Xie, X. (2020). Ultrasound-guided maxillary nerve block via the pterygopalatine fossa: Maxillary artery is the key. *Regional Anesthesia and Pain Medicine*, 45, 1028–1029.

Ruiz Santiago, F., Prados Olleta, N., Tomás Muñoz, P., Guzmán Álvarez, L., & Martínez Martínez, A. (2019). Short term comparison between blind and ultrasound guided injection in morton neuroma. *European Radiology*, 29, 620–627.

Von Coelln, R., Raible, A., Gasser, T., & Asmus, F. (2008). Ultrasound-guided injection of the iliopsoas muscle with botulinum toxin in campocormia. *Movement Disorders*, 23, 889–892.

Wongwattana, S., Kronman, J. H., Clark, R. E., Kabani, S., & Mehta, N. (1994). Anatomic basis for disk displacement in temporomandibular joint (TMJ) dysfunction. *American Journal of Orthodontics and Dentofacial Orthopedics*, 105, 257–264.

Yoshida, K. (2018). Computer-aided design/computer-assisted manufacture-derived needle guide for injection of botulinum toxin into the lateral pterygoid muscle in patients with oromandibular dystonia. *Journal of Oral & Facial Pain & Headache*, 32, e13–e21.

How to cite this article: Bae, H., Lee, Y.-H., Kim, S.-B., Hu, K.-S., & Kim, H.-J. (2025). Ultrasonographic assessment of the lateral pterygoid muscle for BoNT-A injection. *Clinical Anatomy*, 38(7), 780–785. <https://doi.org/10.1002/ca.24220>